2016-9

Scenario Analysis for Techno-Economic Model Development of U.S. Offshore Wind Support Structures

Rick Damiani
National Renewable Energy Laboratory

Andrew Ning
Brigham Young University, aning@byu.edu

Ben Maples
National Renewable Energy Laboratory

Aaron Smith
National Renewable Energy Laboratory

Katherine Dykes
National Renewable Energy Laboratory

Original Publication Citation

Damiani, R., Ning, A., Maples, B., Smith, A., and Dykes, K., “Scenario Analysis for Techno-Economic Model Development of U.S. Offshore Wind Support Structures,” Wind Energy, Sep. 2016. doi:10.1002/we.2021

RESEARCH ARTICLE

Scenario analysis for techno-economic model development of U.S. offshore wind support structures

R. Damiani[1], A. Ning[2], B. Maples[1], A. Smith[1], K. Dykes[1]

[1] National Renewable Energy Laboratory, 15013 Denver West Parkway, Golden, CO 80401, USA

[2] Department of Mechanical Engineering, Brigham Young University, 435 CTB Provo, UT 84602, USA

ABSTRACT

Challenging bathymetry and soil conditions of future U.S. offshore wind power plants might promote the use of multimember, fixed-bottom structures (or "jackets") in place of monopiles. Support structures affect costs associated with the balance of system (BOS) and operation and maintenance. Understanding the link between these costs and the main environmental design drivers is crucial in the quest for a lower levelized cost of energy (LCOE), and it is the main rationale for this work. Actual cost and engineering data are still scarce; hence, we evaluated a simplified engineering approach to tie key site and turbine parameters (e.g., water depth, wave height, tower-head mass, hub height, generator rating) to the overall support weight. A jacket-and-tower sizing tool, part of the National Renewable Energy Laboratory's (NREL's) system engineering software suite, was utilized to achieve mass-optimized support structures for 81 different configurations. This tool set provides preliminary sizing of all jacket components. Results showed reasonable agreement with the available industry data, and that the jacket mass is mainly driven by water depth, but hub height and tower-head mass become more influential at greater turbine ratings. A larger sensitivity of the structural mass to wave height and target eigenfrequency was observed for the deepest water conditions ($> 40\,\mathrm{m}$). Thus, techno-economic analyses using this model should be based on accurate estimates of actual metocean conditions and turbine parameters especially for deep waters. The relationships derived from this study will inform NREL's offshore BOS cost model, and they will be used to evaluate the impact of changes in technology on offshore wind LCOE.

KEYWORDS

offshore wind; jacket substructure; mass sensitivity to environmental variables; balance of system; cost analysis

Correspondence

Rick Damiani,15013 Denver West Parkway, MS3811, Golden, CO 80401, USA

E-mail: rick.damiani@nrel.gov

1. INTRODUCTION

European offshore wind plants have preferred monopile substructures for $3\,\mathrm{MW}$-class turbines because of their ease of fabrication and installation in shallow waters. The U.S. Department of Energy's *Wind Vision* report [1] estimates that $86\,\mathrm{GW}$ of offshore wind could be deployed in the United States by 2050. However, to make offshore wind economically viable in U.S. waters, we must access the high winds located at transitional depths (depths of $30\,\mathrm{m}$–$60\,\mathrm{m}$, and distances of

5 nmi–50 nmi from shore) and utilize larger machines ($\geq$ 6 MW). Preliminary resource assessments for the United States have shown that the transitional-depth resource for Class 4 wind and above exceeds 600 GW [2,3]. As a comparison, the total installed land-based wind capacity in the United States is expected to surpass 70 GW at the end of 2015.

Several studies, e.g., [4, 5], have shown that monopiles, the most readily available solution for shallow waters, are progressively uneconomical or unfeasible because projects are sited in deeper waters and use larger turbine sizes (6 MW+). The challenging U.S. bathymetry and soil conditions might therefore favor fixed-bottom lattice substructures, also known as "jackets," which can more efficiently ensure the necessary structural stiffness. Jackets may also be preferable from a structural reliability and redundancy standpoint when considering hurricane events and hazards associated with waves that are larger than those in most European offshore wind experiences.

In addition to affecting the overall system reliability and performance characteristics, the support-structure design directly impacts capital expenditure (CapEx) via the costs associated with the balance of system (BOS). The substructure and foundation, in fact, are responsible for approximately 14% of the total cost of the offshore wind power plant [6]. When switching from monopiles to jackets, the share of offshore wind power plant costs from the support structure can increase from 15% to 33% [7]. The current variability in CapEx ($3200/kW–$6000/kW [6]) is the largest responsible for the uncertainty in the offshore wind levelized cost of energy (LCOE). The resulting LCOE levels suggest that, to be economically feasible, U.S. offshore wind projects would require power purchase agreement prices to exceed the current wholesale prices [8]. Thus, it is not surprising that the entire offshore wind community is focused on cost reduction [8], for which the support structure represents an area of large opportunity [9,10]. In light of today's political and economic landscape, the 15,650 MW of offshore wind capacity in the U.S. pipeline* make capturing the nexus between support structure costs and the key project parameters crucial for successful deployments [7]. To help stakeholders plan appropriately for the upcoming U.S. offshore wind development, this research seeks to define LCOE trends as functions of site and technology parameters for jacket-based support structures.

Offshore wind projects tend to be designed on a site-by-site basis, and a number of design factors and trade-offs exist [11]. These factors make formulating scaling trends quite difficult. Water depth, wind regime, distance to shore, site geology, wave and current conditions, turbine ratings, turbine inertial properties, and control parameters are a few of the factors that affect the design of an offshore wind turbine and a wind power plant. Some of these parameters together with logistical and manufacturing constraints can drive the design away from the purely mass-optimal solution. On the other hand, innovations in the controls and design choices can favorably curb expected mass and cost trends. To date, no clear assessment of the trends in mass and costs of the support structure as a function of all these factors exists, mostly because of the complexity of the structural problem and the sheer size of the variable and parameter space.

In this study, we propose a bottom-up, engineering methodology to help stakeholders evaluate costs associated with the support structures, and we offer a sample techno-economic analysis to examine the effect of varying turbine ratings, hub heights, water depths, waves, and tower-top masses on the overall support structure design and its mass. Although the engineering approach requires knowledge of site-specific information, it can quickly expose a project's technical trade-offs and costs [11]. The alternative top-down approach, through which mass and cost data from real projects is used to build regression models [11], cannot be readily applied because of the limited existing database, especially concerning jacket-based installations. Therefore, we explored the possibility of extending the engineering approach to assess techno-economic trends among multiple sites and conditions, and we utilized a jacket-and-tower sizing tool to achieve mass-optimized support structures for 81 different configurations.

The paper is organized as follows: the jacket-and-tower sizing tool, part of the National Renewable Energy Laboratory's (NREL's) systems engineering software suite, is briefly described in Section 2 together with the assumptions and simplifications adopted in this study. Section 3 discusses the matrix of numerical experiments and the design philosophy applied to the case studies. Section 4 presents a gallery of the results obtained after post-processing the output of the optimization routine. The economic applicability of jackets is shown to diminish toward deeper water (>45 m) as mass

*Estimated as of June 2015 [8].

gradients sharply increase under the assumed generic turbine parameters and technology constraints; further, the hub height is shown to be more influential toward the overall mass savings than the rotor nacelle assembly (RNA) mass. To show the effect of the approximation in the model inputs, Section 5 presents results from four additional cases that had more detailed information on the metocean conditions and turbine parameters. We show how the originally-derived mass trend still applies below $40\,\mathrm{m}$, but it must be updated for deeper sites, where the optimization results are greatly impacted by specific design conditions. A summary of the key conclusions drawn from this work, and current and anticipated future research efforts are given in Section 6.

2. THE JACKET AND TOWER SIZING TOOL

For offshore wind power plants, a comprehensive approach to the design of the entire wind system is desirable. National Renewable Energy Laboratory (NREL) has developed the Wind-Plant Integrated System Design & Engineering Model (WISDEM™), a wind energy systems engineering toolbox, to help with the the assessment of LCOE and its uncertainty with respect to technological innovations in the various wind power plant components [12, 13]. WISDEM integrates a variety of models including turbine and plant equipment, energy production, operation and maintenance (O&M), and cost modeling [14]. The tool set allows for trade-off studies and guides the design of components as well as the overall system toward a configuration that minimizes the LCOE through multidisciplinary optimization.

Within WISDEM, NREL developed a preliminary sizing tool for support structures (JacketSE), including towers and jacket substructures. The analysis of a multimember structure involves a very large number of design parameters and is more challenging than that of a monopile. Even wind power plant layout aspects, such as turbine array spacing and turbulent wake interactions, can affect the fatigue life of the support structures and thus impact their design. Controlling these factors requires load simulations conducted through coupled aero-hydro-servo-elastic tools, which are computationally expensive and require extensive time to set up and post process. Hence, these sophisticated load simulations are suitable for a phase of the design where only a few configurations are to be assessed. In contrast, JacketSE incorporates a number of simplifications to allow for the rapid analyses of multiple configurations on a personal computer, while searching for an optimal preliminary support structure for given metocean conditions, turbine loading, modal performance targets, standards' design criteria, and select optimization criteria (e.g., minimum structural mass). In this paper, we give an overview of the open-source JacketSE software. For more details on the theory, derivations, and implementation, see [15].[†]

JacketSE is based on a modular code framework written in Python, and it primarily consists of the following submodules: geometry definition; soil-pile interaction; load calculation; finite element solver; structural code check; and optimization. Each submodule is implemented by one or more *components* within OpenMDAO.[‡] The main simplifications in JacketSE lie in the load calculations. Complex hydrodynamics and associated variables (e.g., tidal range, marine growth, and member-to-member hydrodynamic interaction) are ignored, and fatigue assessments are not carried out. These aspects can very well drive the design of certain subcomponents; in particular, the joint cans of the jacket and tower flanges and welds can be driven by fatigue [17–19]. However, it is believed that the main shells are mostly driven by modal and buckling-strength requirements; thus, most of the structural mass should still be captured by the simplified model for the sake of preliminary design assessments and trade-off studies, and with a level of accuracy pertinent to those goals. Additional conservatism can be provided by selecting greater-than-usual drag (c_d) and added mass (c_m) coefficients, by choosing a worst-case loading scenario, and by additional safety factors (see also Section 3).

The coupled geometry components include (see also Fig. 1a) piles, legs, mud-brace, x-braces, top-brace, transition piece (TP), and tower.

[†] The code has also been open-sourced and the program, tutorials, and theory can be found at `https://github.com/WISDEM` and [15, 16].
[‡] National Aeronautics and Space Administration software for multidisciplinary analysis and optimization, `openmdao.org`.

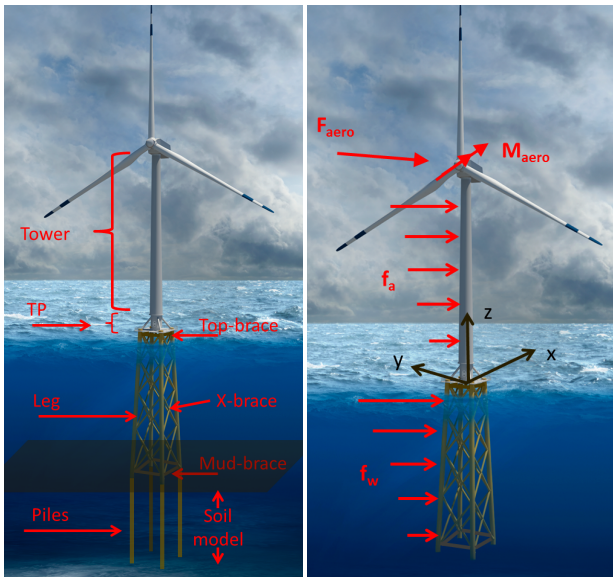

Figure 1. (a) JacketSE's main geometric and structural component groups; (b) main coordinate system used by JacketSE, principal sources of loading, and their general areas of application. Modified from an illustration by Joshua Bauer, NREL.

A series of inputs are needed to define the entire geometry. Some of these inputs are parameters (i.e., they won't change throughout an optimization process), whereas others can be defined as design variables to be optimized. For example, the water depth, the number of legs and brace levels (bays) for the jacket, the height of the deck above mean sea level, and the hub height are fixed parameters; the batter, the pile embedment length, the deck width, the tower-base and tower-top diameters, the tower-waist height, and the outer diameters and wall thicknesss for piles, legs, and braces are some of the key geometric variables that the tool can output.

The software determines the three-dimensional coordinates of the joints based on all the inputs, and it further subdivides each member into multiple beam finite elements.

The soil-pile interaction component interacts with the piles' module and calculates the pile-head equivalent stiffness and the necessary embedment length for the given pile-head loads. Parameters to be input for the soil submodule include the stratigraphic schedule of undrained shear strength, friction angles, and specific weight.

The soil model generally assumes a linear trend of the soil modulus with depth below the seabed, which is typical of consolidated clays. For cohesionless soils, corrections are employed in the calculation of the pile-head stiffness. Equivalent spring constants to be applied as boundary conditions at the seabed nodes in the finite-element analysis model [15] are calculated based on the work by [20–22]. The pile axial-capacity verification is based on [23].

JacketSE treats all loads as pseudo-static and considers two design load cases (DLCs), usually taken as (1) an operational DLC (similar to DLC 1.6 from [24]) and (2) a parked DLC (similar to DLC 6.1 from [24]). This approximation reduces computational time and resources, but it does not retain the accuracy of aero-elastic load simulations. For this reason, loads and partial safety factors (PSFs) must be selected with care to compensate for the lack of a fully dynamic treatment.

The loads that are considered by JacketSE are permanent actions (dead loads) and live loads. Dead loads are the gravitational loads associated with the self-weight of the structure and the so-called secondary steel, among which are tower internals, platforms, boat landing, anodes, and deck appurtenances such as transformers and cranes. Secondary steel can be approximated by lumped masses at tower nodes and at the center of the TP deck. Applying a fictitious, increased steel density for the jacket and the tower can help simulate the inertial effects of hardware, cathodic protection, corrosion allowance, and coatings.

The live loads include aerodynamic loads from the RNA (prescribed as fixed inputs in this study), drag loads from the wind on the support structure, and hydrodynamic loads. Figure 1b shows the approximate location of the live loads' application points.

The aerodynamic drag on the tower and jacket members above water is approximated using two-dimensional drag theory and a power-law wind profile [24] with prescribed shear and wind speed at hub height. Two values for the drag coefficient are input as parameters: $c_{d,at}$ for the tower and $c_{d,aj}$ for the substructure. These coefficients must account for the dynamic amplification (gust) factors (e.g., [25–30]). Because no aerodynamic force is computed for the cross members and the TP, the $c_{d,at}$ and $c_{d,aj}$ should be further augmented to account for the load contributions from these members.

Under water, hydrodynamic loading was calculated using the well-known Morison equation for slender members and Airy theory, which does not consider wave stretching [15, 31, 32]. The coefficients $c_{d,wj}$ (water drag coefficient) and c_m (added mass coefficient) are selected depending on the conditions of the specific DLC under consideration [15]. Additionally, the hydrodynamic loads are solely calculated on the main leg members. To include the effects of cross-brace loading and to mitigate the absence of wave stretching, the phase difference between the maximum wave speed and acceleration is ignored, and larger-than-normal hydrodynamic coefficients can be applied. Note that the jacket legs are assumed to be flooded, and thus hydrostatic effects are ignored for the leg members; whereas sufficient strength over hydrostatic effects for the mud- and cross-braces is verified by applying a set of semiempirical engineering rules (see below).

The finite-element analysis solver at the core of JacketSE (called pyFrame3DD) is a modified version of FRAME3DD [33], which is based on Timoshenko beam elements [34, 35]. All of the external loads are reduced to forces applied at the element nodes, where material utilization-ratio calculations are also performed.

The utilization ratio is derived from the generic ultimate limit state structural verification, which can be expressed as in Eq. (1) [36]:

$$\gamma_f F_k \leq \frac{f_k}{\gamma_n \gamma_m} \tag{1}$$

where F_k is the unfactored characteristic load; f_k is the material-unfactored resistance; γ_n is the consequence of failure PSF (or importance factor based on the redundancy and fail-safe characteristics of the various components); γ_f is the generic load PSF; and γ_m is the material PSF. The design standards provide recommended values for γ_f and γ_n [23, 24, 36–39] as well as γ_m [36, 40–43]. JacketSE recasts Eq. (1) in utilization equations for the tower and the substructure, and it returns values for the utilization ratios. Ultimate limit state structural verification amounts to ensuring that the material utilization ratio is below one. For example, the tower is verified if the utilization ratios are less than one at all the tower element nodes, that is, the stresses are kept below the allowable yield strength, and stability is guaranteed both at a global and local level. For the jacket, utilization ratios are calculated at the member and joint level following the criteria in [23]. The members are checked for tension and for combined axial compression and bending; whereas the joints are verified by considering the loads from the intersecting members (see [15]).

The x-braces and mud-braces must also satisfy a few additional stiffness and strength criteria (see [15]) that are derived from engineering experience [44]. These constraints, which are also expressed as utilization ratios, are based on the relative dimensions between braces and legs, and they ensure a rigid truss behavior of the individual jacket bay and therefore an adequate shear transfer from one leg to another; the manufacturability of the brace with associated positive buoyancy; and adequate hydrostatic strength.

As mentioned earlier, JacketSE can be used in combination with various goal-seeking schemes through an optimization module.[§] The primary algorithm used in this research was constrained optimization by linear approximation (COBYLA) [45], a direct search method as implemented in Python. This algorithm was chosen in part because of the numerical noise associated with nested solvers, which hampered the use of a pure gradient-based method in some of the cases analyzed. Further, because reasonable initial guesses were known from engineering understanding, a local direct search method

[§] For more details on the available OpenMDAO drivers and algorithms refer to openmdao.org

worked rather well by producing converged results relatively quickly. For a subset of the cases, however, we confirmed convergence against the results obtained via Sparse NOnlinear OPTimizer (SNOPT) [46], a sparse sequential quadratic programming method. Because of the modularity of the software, the COBYLA optimizer could be swapped with better methods as new, more refined analyses are carried out.

For this research, the objective function was defined as the total mass of the support structure, and the design-variable acceptance ranges were based on manufacturability constraints (e.g., minimum and maximum values for the jacket batter, tower-base and tower-top diameters, member diameter-to-thickness ratios, pile length, and deck width). Other constraint functions were set to ensure certain performance characteristics—for example, to limit the footprint at the seabed, to guarantee the first eigenfrequency within an acceptable range, and to ensure material utilization below unity. The final accuracy in the optimization and the feasibility tolerance were set at 10^{-3}.

3. APPROACH TO THE CASE STUDY

In this study, we analyzed a simplified loading scenario with two key DLCs: a parked case and an operational case. To investigate other DLCs, more detailed information on the load entities from the RNA is required, which was not available at the time of this study. Although a parked DLC was considered (with coaligned loads from 50-yr wave and wind gust), it did not appear to drive the design for the cases analyzed. This is likely because the turbines were of International Electrotechnical Commission (IEC) Class II [36] (thus, they were not subject to extreme wind gusts greater than $59.5\,\mathrm{m/s}$). Class II was selected to analyze an average behavior rather than to try to capture extremes within this initial techno-economic analysis. For the same reason, hurricane conditions were ignored. The remainder of the data and results presented in this paper are for the operational DLC considered, which is representative of the DLC 1.6 in [24]. For this DLC, the maximum expected turbine-rotor thrust and the load from a 50-yr wave were assumed to be aligned along the jacket-base diagonal—that is, along two nonadjacent piles.

The objective function was to minimize total mass including that of the tower, four-legged jacket, TP, and piles. As further described below, the constraints were set based on expected manufacturing and logistic limits, on component utilization less than unity, and on a soft-stiff approach for the modal performance.

The target first natural frequencies (f_0) for the various cases analyzed were chosen to be above the rotor-forcing and below the blade-forcing frequencies (soft-stiff approach); a lower bound was set at $0.21\,\mathrm{Hz}$ to prevent resonance excitation from wave forcing (cf., [47]). In most cases, the obtained eigenfrequency was allowed to lie within $[f_0, 1.05 \cdot f_0]$.

In this study, the piles were sized solely based on the axial capacity requirement. The pile surface area must be sufficient to develop the necessary friction to overcome the axial load transferred by the jacket leg. Pile behavior was considered as unplugged, which almost doubles the available surface area capacity. Pile embedment length is a trade-off between steel mass and installation costs. In general, longer pile penetrations require longer time spent at sea and are economically justifiable for deeper installations, but they are likely not viable for the shallower water sites. Embedment length bounds were selected to try to capture these trade-off aspects.

For the substructure, $c_{d,wj}$ and c_m values (2 and 4, respectively) were approximately doubled with respect to those recommended by [23], and wave loads calculated on the main legs were multiplied by a factor of four to include hydrodynamics effects on secondary members and lack of wave stretching. For the tower and the above water jacket members, values of $c_{d,at} = 2$ and $c_{d,aj} = 4$ were chosen to account for TP wind drag, and we included a gust factor of 1.2. Preliminary comparisons of JacketSE-calculated loads to the peak loads from dynamic simulations performed using SACS (a commercial package by Bentley for the analysis of offshore fixed-bottom structures) and FAST v8 (NREL's aeroelastic tool) for similar substructure configurations led to the choice of those coefficients. The power law, wind shear exponent was set at 0.11.

The material assumed for all components was ASTM 992 steel (E=$2.1 \times 10^{11}\,\mathrm{Pa}$, ν=0.3, f_y=$345\,\mathrm{MPa}$ [48]), and its density was augmented (ρ=$8740\,\mathrm{kg/m^3}$) for what was stated in Section 2. In the absence of known specific geotechnical

Table I. Stratigraphy assumed in this study.

Depth (m)	γ_s [a] ($\mathrm{N\,m^{-3}}$)	ϕ_s [b] (°)	δ_s [c] (°)
-3	10,000	36	25
-5	10,000	33	25
-7	10,000	26	25
-15	10,000	37	25
-30	10,000	35	25
-50	10,000	37.5	25

[a] effective soil density
[b] angle of internal friction
[c] steel-to-soil friction angle

Table II. Baseline turbine parameters.

Turbine rating	Unfactored peak thrust	Unfactored torque at max thrust	Gust wind speed at max thrust	RNA mass	Rotor diameter	Hub height	Target system first eigenfrequency
MW	kN	kN m	$\mathrm{m\,s^{-1}}$	t	m	m	Hz
3 (Class II)	507	2303	33	234	113	80	0.26
6 (Class II)	1014	6522	33	500	160	103.5	0.21
10 (Class II)	1687	13995	33	900	206	126.5	0.21

conditions, a sandy, average-stiffness soil with fixed stratigraphy, as shown in Table I, was selected for all the sites. The load PSFs were set at 1.35, except for gravity loads (1.1) [36, 49]; material, importance, and buckling PSFs were set at 1.1 [23, 49, 50]; for the pile embedment length calculation, a value of PSF=1.25 was selected [39, 51].

3.1. Variables and Parameters Specific to the Individual Case Studies

In the absence of publicly available turbine reference models, we derived the turbine geometric and performance parameters from experience gained from previous offshore projects. Table II shows the key parameters for this study. Some of the original parameters were scaled to approximately match IEC Class II [24] machines with power densities of about $300\,\mathrm{W\,m^{-2}}$. The shown values for thrust and torque include dynamic effects for the presence of gusts and structural response above rated conditions, and they were further factored by JacketSE during the optimization calculations. These loads are largely affected by the control system strategy and parameters; therefore, they can vary largely from one turbine to another. Here, the controllers used to derive the loads were not optimized but simply scaled with machine size from a simple baseline similar to that described in [52]. Other components of the RNA loads were also included in the calculations, (e.g., the yaw moment, which has implications on brace sizing), but they had a slightly lesser impact on the results and are not shown.

The values of f_0 shown in Table II represent the modal performance requested for the various system layouts. For a few cases, the upper bound of the frequency acceptance band (discussed above) had to be relaxed to find feasible configurations (see Section 4).

Table III lists the range of the metocean parameters that were considered. Three sites—with water depths of 20 m, 40 m, and 60 m—were identified together with associated 50-yr maximum wave heights and periods. The deck height above the still water level was calculated to clear the maximum wave crest with an additional air gap of 1.5 m (per [23]). The wave crest height was based on the 50-yr wave heights (a mean multiplicative factor of 0.65 was used following Table 4.2.3 per [37]), a tidal range of 2 m, a 50-yr surge of 2 m, and a lowest astronomical tide level of -1 m mean sea level. A

Table III. Main simulation sweep parameters. Hub height and RNA mass were combined in all cases, whereas three sets of other parameters were considered linked to water depth.

Parameters	Units	Values		
Hub height	Times the baseline value	1	1.15	1.3
RNA mass	Times the baseline value	0.8	1	1.2
Water depth	m	20	40	60
50-yr wave height	m	15	22.5	30
50-yr wave period	s	10.1	12.15	14.2
Deck height	m	14.25	19.12	24

uniform current of $0.5\,\mathrm{m\,s^{-1}}$ speed was added for all cases. These conditions are loosely representative of sites along the mid-Atlantic.

As indicated in Table III, the turbine RNA masses were varied by $\pm 20\%$, and the hub heights were varied by up to 30% of their respective baseline values. The baseline hub heights were regarded as the minimum acceptable values based on the selected deck heights and clearance among blade, deck, and water level.

By combining the various environmental and turbine parameters, 81 different configurations were identified (three water depths x three turbine ratings x three hub heights x three RNA masses). Some system configurations are on the extreme end of what would be considered a viable spectrum—for example, maximum hub height and turbine rating combined with minimum water depth—yet they were deemed sufficient to describe a reasonable envelope of potential offshore installations in U.S. waters.

For each of the 81 sets of design parameters, valid ranges of the design variables were identified based on manufacturability constraints and industry experience. For example, leg and brace minimum wall thickness was set at $0.0127\,\mathrm{m}$ (half inch), and leg outer diameter was varied between 0.8–$2.5\,\mathrm{m}$. Pile lengths were limited to 50–$70\,\mathrm{m}$, depending on water depth. The substructure footprint (distance between two adjacent piles) was allowed to grow with water depth and turbine size (maximum values ranged from 30–$40\,\mathrm{m}$). All of these choices on variable and parameter ranges were made to try to keep the comparison as fair as possible among the 81 configurations so that conclusions could be reached and trends identified without excessive forcing by the designer's choices. In some cases, no feasible solution could be obtained without bending some of these constraints. For example, in the case of maximum turbine rating and hub heights, the tower-base diameter upper bound was relaxed from $8\,\mathrm{m}$ to $9\,\mathrm{m}$. Also, for the deepest water depths, five bay jackets were considered; four were considered in all other cases.

Finally, a lumped mass (100–$200\,\mathrm{t}$ depending on turbine size) was added to the TP to account for deck flooring, railing, boat landing, and secondary appurtenances.

4. RESULTS OF THE ANALYSIS

The database[¶] built through JacketSE allows for the investigation of a large number of output parameters (e.g., geometry characteristics and mass of the various components), but only trends of the support structure mass, piles' properties, jacket footprint, and tower mass are discussed in this paper.

4.1. Substructure Mass

A summary of the model results is plotted in Fig. 2, wherein the total support structure mass (including the piles and the tower) and the jacket mass are shown as a function of turbine hub height and water depth. Bilinear interpolation surfaces

[¶]The entire database is available upon request by contacting the NREL.

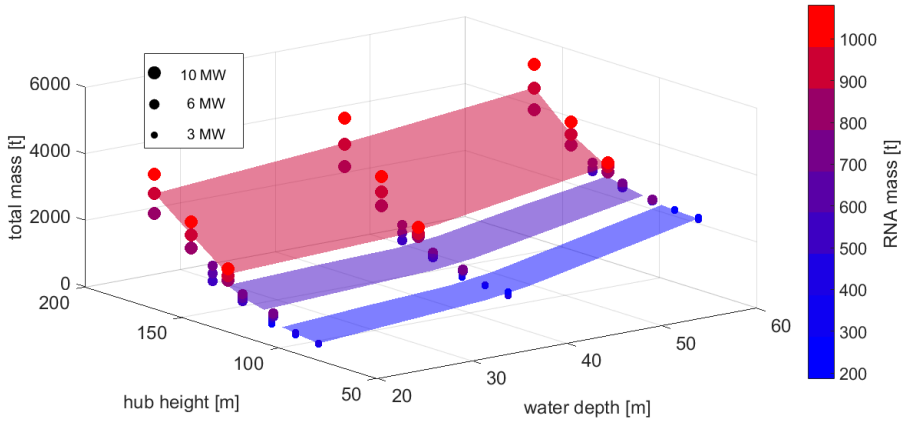

(a) Total support structure mass

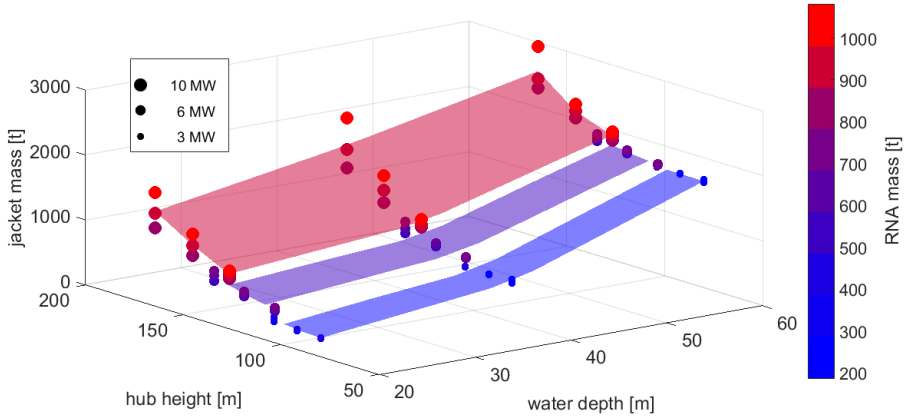

(b) Substructure mass

Figure 2. Overview of the structural mass trends. The turbine rating is indicated by the different size of the symbols (which in some cases overlap). The RNA mass is shown by the color map. The surfaces are bilinear interpolations of the data grouped by turbine ratings.

are also shown in the figures; in case of overlapping x or y coordinates of the data points, these are averaged before the interpolation.

The trends shown in Figs. 2a and 2b are similar, and one may observe that the hub height is more influential for the larger turbine sizes and for water depths greater than $40\,\mathrm{m}$. The RNA mass is less influential at the smaller sizes (as also shown by [53]), but it becomes progressively more important at higher hub heights and with larger turbine ratings. This can be justified by considering the requested modal performance, which is directly affected by both the tower length (hence hub height) and tower-top mass. In Fig. 3, the jacket-mass-vs.-hub-height trend is shown for different water depths, together with best-fit polynomial curves. At a water depth of $60\,\mathrm{m}$, hub-height effects are secondary except for the 10-MW turbines. In shallower water sites, the variation of mass with hub height is more significant above heights of $100\,\mathrm{m}$, which also suggests that the current installations (mostly hub heights below $100\,\mathrm{m}$) are largely driven by hydrodynamic loads.

A close examination of Fig. 3 shows how, for the 3-MW ratings, the gradient of the jacket mass with respect to the water depth and hub height is dominated by the water depth component. The gradient magnitude, not shown here for the sake of brevity, increases from $0.10\,\mathrm{t\,m^{-1}}$ at a depth of $20\,\mathrm{m}$ to $0.19\,\mathrm{t\,m^{-1}}$ at a depth of $60\,\mathrm{m}$. For the bottom two water depths, a slight increase in mass can be observed between hub heights from 92–$104\,\mathrm{m}$, at a water depth of $60\,\mathrm{m}$, the jacket

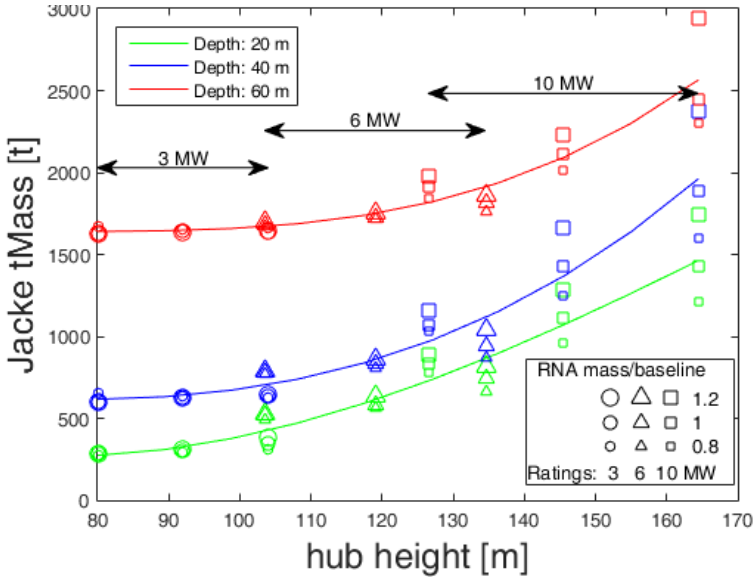

Figure 3. Jacket mass as a function of hub height for different water depths (different symbol colors) and best-fit polynomial curves. More details on the symbols used are given in the legend.

mass is virtually unchanged, and the code returned slightly lighter jackets for the heavier RNAs. This information is more clearly depicted in Fig. 4a, wherein the jacket mass, made dimensionless with the average value among all of the 3-MW cases, is plotted as a function of hub height for the subset with a water depth of 60 m. This apparent contradiction is due to the assumed eigenfrequency constraint. Although the code tries to satisfy strength criteria, it also attempts to increase the jacket footprint. A wider footprint, in a battered configuration, transforms some of the shear load into axial load at the main legs, thus reducing the bending stresses and more efficiently utilizing the material. However, the wider footprint also raises the first natural frequency of the system. As shown in Fig. 4b, the lightest RNAs at the deepest water level produced eigenfrequencies in excess of 0.3 Hz, well beyond the allotted 5% band above the target frequency. In fact, except for the heaviest RNAs at the highest hub heights, the code did not find a feasible solution for the 3-MW cases at a depth of 60 m and at the set target eigenfrequency. Relaxing the frequency upper bound led the code to finding feasible but heavier solutions. In other words, in an attempt to reduce the configuration's natural frequency, the code could not help but find solutions that featured heavier jackets than those associated with heavier RNAs. In this case, in fact, a larger RNA mass is beneficial because it helps reduce the system eigenfrequency toward the requested target. A similar effect is associated with higher hub heights, although it is mitigated by the increased overturning moment: for this reason, the order of the data points in Fig. 4a changes for the largest hub height, but it does not completely reverse. This aspect can be important in cases with very light RNAs and should be revisited, although it is not expected to be an issue with larger machines envisioned in future offshore wind power plants.

Turning now to the mass gradient associated with the 10-MW rating cases, Fig. 3 shows how the hub height is as influential as the water depth at shallow depths but slightly less important for the deepest sites and for lower hub heights. Overall, the magnitude of the gradient (not shown) is lower than that for the 3-MW cases, and it ranges from $0.06\,\mathrm{t\,m^{-1}}$ at a depth of 20 m to $0.09\,\mathrm{t\,m^{-1}}$ at a depth of 60 m and for the greatest hub heights. The decreasing gradient magnitude with ratings increasing from 3 MW to 10 MW signifies that the environmental parameters become less influential for larger turbine sizes, for which the RNA loads are the key support-structure drivers. This is also shown in Fig. 3; note how the points get closer together between the middle and deepest water levels around hub heights of 140 m, but farther apart for higher hub heights.

Data from actual installations and other consultancy studies [10,54] that have publicly available predictions on structural steel quantities were used for comparison and validation of our results. These data points are plotted in the graphs of Fig. 5.

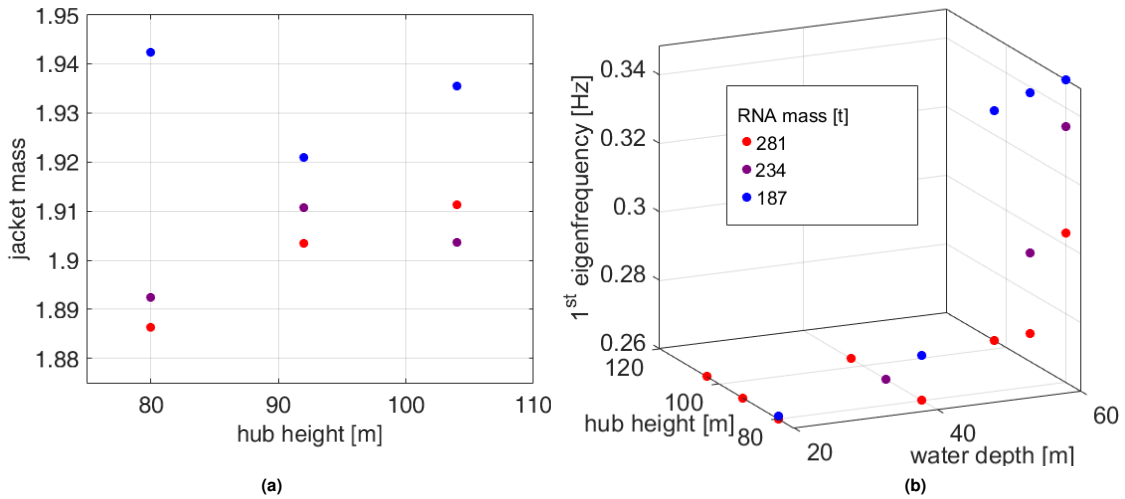

Figure 4. 3-MW turbines: (a) jacket mass as a function of hub height at water depth of $60\,\mathrm{m}$ made nondimensional with the average mass among all the 3-MW cases (note that the spread is exaggerated by the y-axis scale); (b) system's first natural frequency as a function of water depth and hub height. The colors denote RNA mass as indicated by the legend in (b).

In that figure, the surface that interpolates our calculated data was extrapolated toward lower hub heights and water depths to compare to the available industry data. As shown, the model agrees relatively well (errors below 12%) with the industry data for water depths between 20–$40\,\mathrm{m}$, but it underestimates (35% error) the installation data points for shallower sites. The model also returned a large gradient of the jacket mass with respect to water depth above $40\,\mathrm{m}$ and below $10\,\mathrm{m}$, which is partially caused by the lack of resolution around 45–$50\,\mathrm{m}$ and below $20\,\mathrm{m}$. A larger scatter is shown, however, when model data points are compared to other consultancy predictions. This is further discussed in Section 5.

4.2. Pile Mass and Embedment Length

In Fig. 6, we show the obtained trends in piles' mass and embedment length. Because of the assumed, nonuniform soil conditions, the diameter and the length of the pile do not have the same exact weight on the pile axial capacity, though both contribute to the friction-generating surface area. An upper bound to the embedment length was set proportional to water depth as explained in Section 3, and Fig. 6a shows that most solutions bumped against this constraint. When compared to the industry data, the calculated piles' mass was underestimated by up to 50%. Part of this discrepancy can be ascribed to an optimistic choice of soil conditions and PSFs. As mentioned in Section 3, a safety factor of 1.25 on soil conditions was used based on [38, 39, 51]. The new American Petroleum Institute [23] and American Bureau of Shipping [55] standards recommend higher safety factors (1.5-2) for pile design. Another factor that may affect these results is linked to having the pile diameter as a continuous variable in the optimization runs, whereas, in practice, standard stepwise sizes should also be considered.

Note also how the pile mass is affected by the modal constraints and the maximum-footprint constraint imposed on the various configurations (see also Section 4.3). The wider the jacket base, with everything else being equal, the lesser the axial load on the pile. Additionally, as already mentioned, a wider footprint tends to increase stiffness and natural frequencies. With shorter and shorter hub heights (shorter and stiffer towers), a narrower base must be devised to match the target first system eigenfrequency (e.g., $0.26\,\mathrm{Hz}$ for the 3-MW turbines), but at the cost of heavier piles. The trend in the pile mass for the smallest turbine sizes (see Fig. 6b) is affected by this behavior, and it becomes more significant as the RNA mass gets lighter.

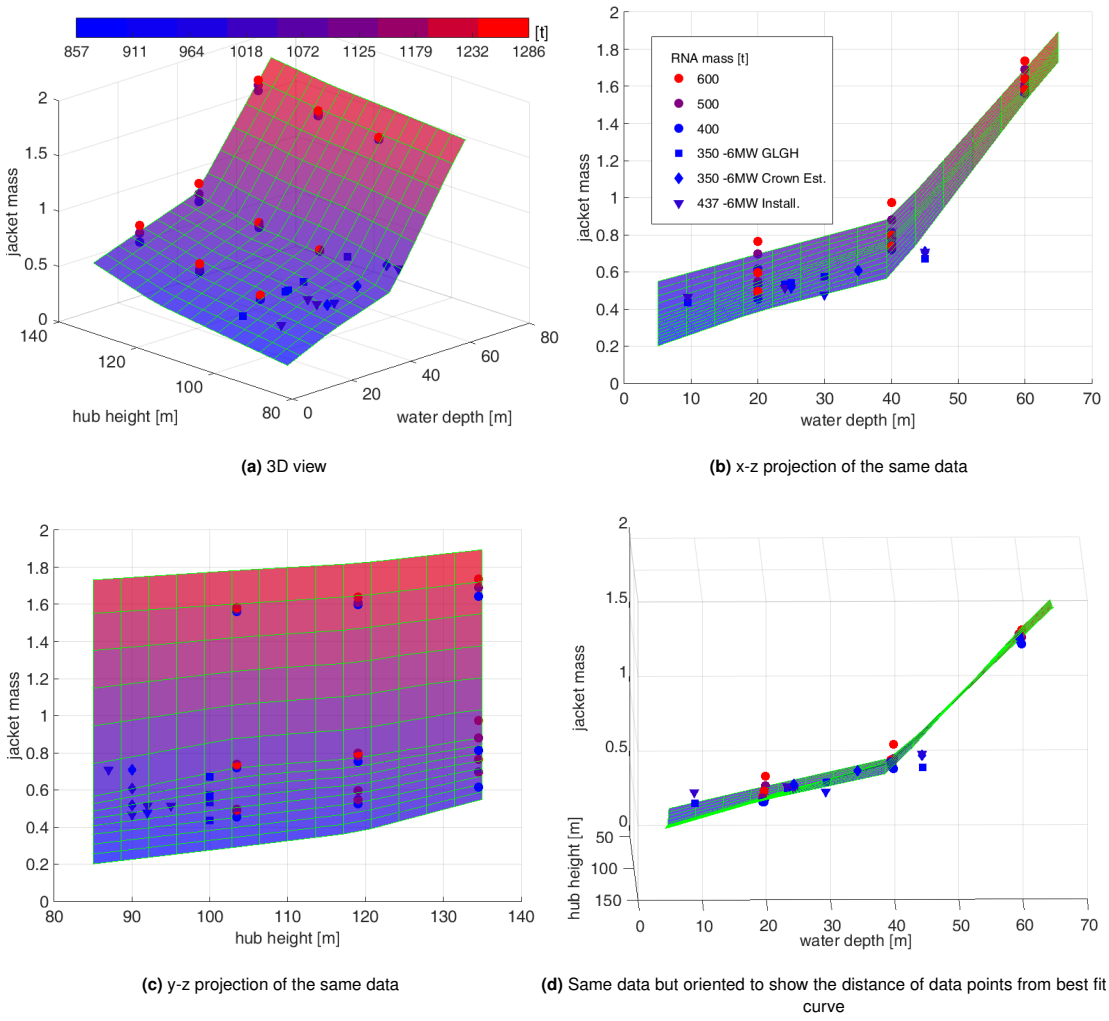

(a) 3D view

(b) x-z projection of the same data

(c) y-z projection of the same data

(d) Same data but oriented to show the distance of data points from best fit curve

Figure 5. Jacket steel mass trend for the 6-MW turbine cases. The study data points are denoted by filled circles, with colors indicating RNA mass as denoted by the legend in (b). The surface (bilinear interpolation of the 81 data points) is color coded by jacket mass tonnage, and the legend is given in (a). In all the plots, the z-axis shows jacket mass made nondimensional with its average across all the 6-MW cases. Other symbols indicate: existing installations of 6-MW offshore turbines (triangles), predictions from the Crown Estate study [10] (diamonds), and predictions from [54] (squares).

4.3. Jacket Footprint

The footprint calculated for the various configurations is shown in Fig. 7. The general trend shows a strong dependency on water depth and hub height; however, the prescribed footprint constraints, which were based on assumed transportation requirements to make the installations economically viable, prevent us from further conclusions. For the deepest sites, the optimization pushes the footprint to the maximum allowed values except for the lowest hub height cases. Generally speaking, a wider base makes the structure stiffer and more efficient, and, for the lightest turbines, a narrow base is necessary to avoid overshooting the target eigenfrequency. If the modal performance constraint were to be relaxed, results would obviously change with consequences on overall structural mass, and this should be the object of future investigations.

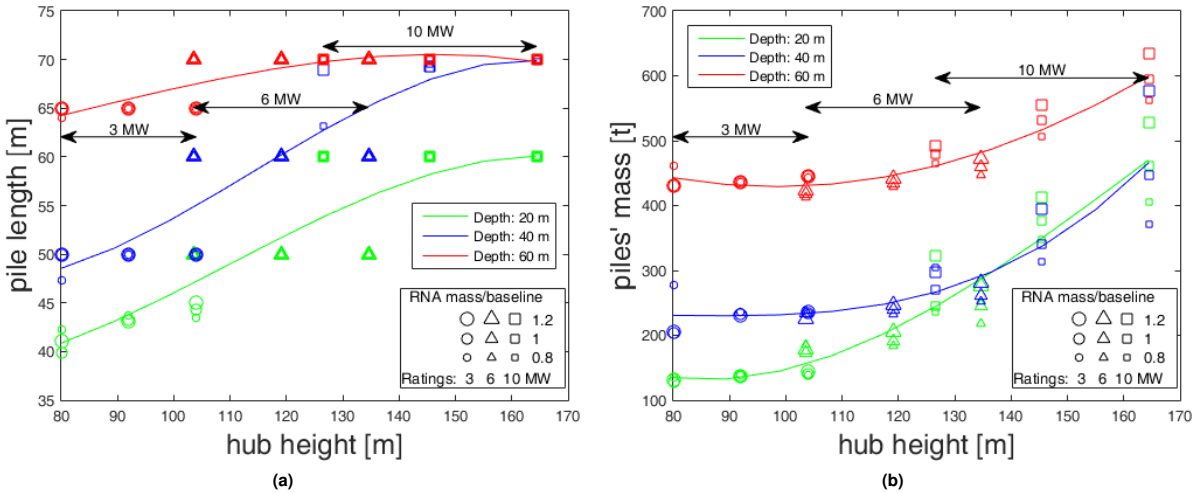

Figure 6. Piles' embedment length (a) and mass (b) as a function of hub height for various water depths, and best-fit polynomial curves. More details on the symbols used are given in the legends.

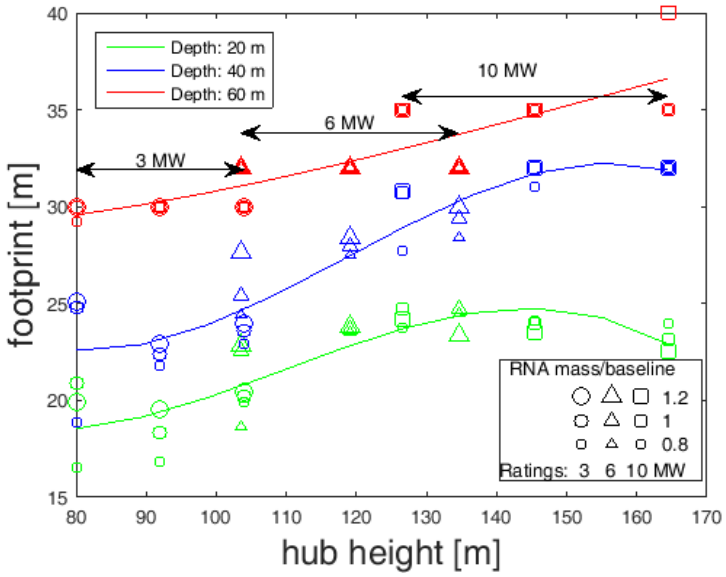

Figure 7. Footprint at mud line as a function of hub height for various water depths, and best-fit polynomial curves. More details on the symbols used are given in the legend.

4.4. Tower Mass

The tower mass (see Fig. 8) is obviously mostly dependent on hub height and turbine rating, which drive modal characteristics and loads. The RNA mass has a secondary effect, but it becomes more important at larger turbine ratings, again driving the modal properties of the system. The water depth has an indirect impact on tower mass, which seems lower at larger water depths than at shallower depths. This is because deck heights were selected to clear the 50-yr wave crest elevations, which are proportional to water depth for the sites analyzed in this study, and therefore deeper water sites required shorter towers. Additionally for the largest turbine ratings, tower base diameters were allowed to grow to 9 m, which allowed for more efficient designs with smaller wall thicknesses.

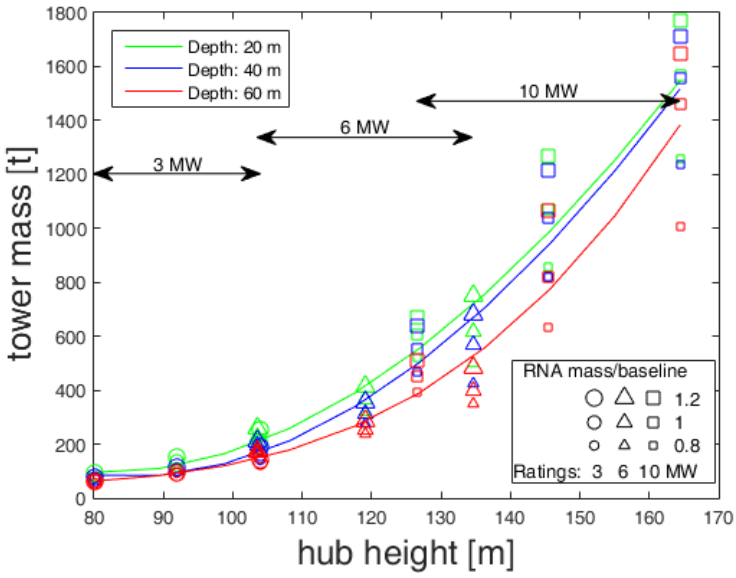

Figure 8. Tower mass as a function of hub height for various water depths (color coded), and best-fit polynomial curves. More details on the symbols used are given in the legend.

5. A SNAPSHOT INVESTIGATION OF THE SENSITIVITY OF THE MODEL TO THE INPUTS

As noted in Section 4.1, some scatter still exists among industry data and model-derived data. Differences exist both among the installation data themselves and among those and the predictions from various consultancies' models. For instance, for the jacket mass, at a water depth of $45\,\mathrm{m}$, our prediction is only 5% greater than the actual installation data, but it is some 35% larger than the data calculated by [54]; at a water depth of $30\,\mathrm{m}$, our prediction differs by 12% from the installation data; whereas [54]'s prediction differs by 20%. Overall, there is more concern for sites in the deepest waters, where the relative errors are larger.

As already mentioned, part of the discrepancy is attributable to the lack of resolution in the model and in the cases analyzed. Another possible explanation lies with the choices of input parameters to the various models (JacketSE and other industry predictive models). To further evaluate the sensitivity of the chosen site and turbine parameters and modal constraints, we ran additional optimizations with new parameters. This time, the data were taken from actual project studies: the metocean data were derived from the National Oceanic and Atmospheric Administration's (NOAA's) buoy database, and the turbine data were derived by design calculations for a 6-MW machine directly performed by its original equipment manufacturer (OEM). The relevant parameters are shown in Table IV. The inputs between these and the original dataset cases differed in the values of hub height, peak thrust, maximum wave height, lumped mass at the TP, and target modal performance.

Figure 9 displays the results of these simulations (denoted by hollow triangles) in terms of substructure mass and in the same space as the previous data. It can be observed that the first two data points, at water depths below $40\,\mathrm{m}$ are well aligned with the predicted trend of our study. This lends confidence in the obtained results and the approach taken for that region, even though only approximations of the various metocean and turbine parameters were used.

However, the last two data points (at water depths of $50\,\mathrm{m}$ and $65.8\,\mathrm{m}$) are largely overestimated (by 25% and 100%, respectively) by the previously assumed interpolating surface. This difference indicates that the model is highly sensitive to the input parameters for water depths larger than $40\,\mathrm{m}$, and care must be exercised when techno-economic analyses are to be performed in that domain.

Table IV. Metocean parameters for actual buoy sites[a] and OEM-provided 6-MW turbine data.

Metocean Parameter	Units	Site/Buoy No.			
		Frying Pan Shoals (NC)/41013	Long Island (NY)/44025	WIS Cape Cod (MA)/W63067	SE Nantucket (MA)/44008
Water depth	m	23.5	40.8	50	65.8
50-yr wave height	m	18.33	17.6	17	23.3
50-yr wave period	s	13.3	12.5	13.6	11.2
Deck height	m	13.2	16	15.4	16.9
Turbine Parameter	**Units**	**Values**			
Hub height	m	97			
RNA mass	t	365			
TP lumped-mass	t	75			
Unfactored peak thrust	kN	1937			
Unfactored torque at max thrust	kN m	5350			
Gust wind speed at max thrust	m/s	20			
Target system first eigenfrequency	Hz	0.28			

[a] Metocean data were from: National Oceanic and Atmospheric Administration (NOAA), National Data Buoy Center, http://www.ndbc.noaa.gov; U.S. Army Corps of Engineers, Wave Information Studies, http://wis.usace.army.mil

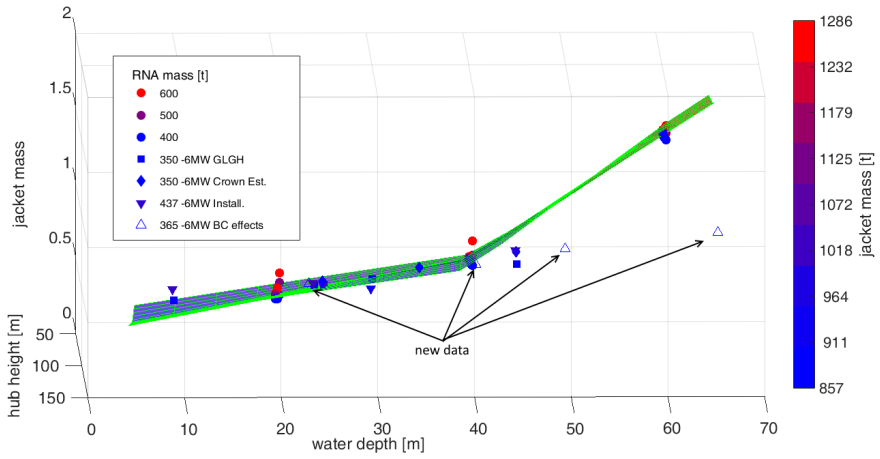

Figure 9. As in Fig. 5d, but with additional data points (hollow triangles), associated with the conditions shown in Table IV. The arrows point to the new data for clarity.

6. DISCUSSION OF THE RESULTS AND FUTURE WORK

The primary motivation of this research lay in determining key relationships between environmental design drivers and costs associated with wind power plant BOS, of which the support structure is the primary driver. We wanted to test the capability of a bottom-up approach toward techno-economic analyses. The alternative top-down approach is challenging given the fledgling status of the offshore wind industry, especially in the United States, which hampers the extraction of reliable regression curves from the limited project data.

The study examined the effect of varying turbine ratings, hub heights, water depths, wave heights, and tower-top masses on the overall support-structure mass. Because of the emphasis toward U.S. installations, lattice substructures,

or jackets, which are expected to be preferable to monopiles in U.S. waters, were the focus of this research. The analyzed turbine ratings ranged from 3–10 MW; the hub heights ranged from 80–165 m; and the water depths for three idealized sites ranged from 20–60 m. Turbine parameters (weights, inertial properties, and loads) were derived from scaling approximations of existing offshore turbine models. As a result, 81 configurations were selected within the space of environmental variables that current and future offshore projects may envision for fixed-bottom installations.

We used JacketSE, a computer-aided engineering tool within NREL's systems engineering WISDEM toolbox, to determine preliminary mass-optimized configurations for each case. Despite JacketSE being based on a simplified treatment of the physics, it delivered results in reasonable agreement with the data available from the industry and current installations, especially at water depths less than 45 m.

The output data included geometric parameters for main lattice, TP, tower, and piles, as well as their respective mass schedules. Although we offered a snapshot of the calculated tower mass, footprint, and pile property trends, we concentrated our analysis on the mass trends of the jacket and piles because these are deemed the best proxy for the costs of support-structure installations at sea.

A number of complex relationships emerged from the data, emphasizing how the interdependencies among environmental parameters, assumed target performance, and structural constraints have important consequences on the derived trends. General conclusions drawn from these studies include:

- Water depth was the main driver for the jacket and support structure mass. As turbine ratings increase, however, hub height and tower-top (RNA) mass were more important factors on the overall support mass. The higher the hub height, the more influential the change in RNA mass becomes.
- At the lowest turbine ratings, the lattice mass can decrease with increasing hub height and tower-top mass. In these instances, the design included stiffer and heavier towers, leading to the combined tower/substructure mass increase, as expected. If the tower and substructure were designed independently rather than in an integrated manner, as done in this study, it is likely that the increase in mass would be more substantial and that no substructure-related savings would be attained.
- A change in support-structure mass gradient is expected around water depths of 45–50 m, under the assumed geometry, parameters, and general layouts.
- The tower mass trends were as expected, with hub height and turbine rating as the main drivers and the RNA mass playing a lesser role.
- Piles' mass and footprint were constrained by modal performance. The lighter turbine masses and shorter hub heights required narrow jacket bases to achieve the target eigenfrequencies but at the cost of heavier piles. A large difference was noted between the calculated and the actual installation piles' mass. Although this could be partially attributable to the choice of soil conditions and safety factors, it is an aspect that needs further investigation.

Some of these conclusions are highly dependent on the combination of environmental factors and design constraints. If the modal performance (e.g., resonance avoidance) could be guaranteed via a dedicated control system design, the trend of structural mass for the lattice and foundations would change because one could take advantage of further mass savings. Additionally, if some of the manufacturing constraints or transportation constraints (namely tower diameters, diameter-to-thickness ratios, and substructure footprints) could be relaxed by incorporating new technological advancements and installation strategies, new mass and LCOE trends could be identified.

For validation purposes, we compared results in terms of substructure mass to the limited data points from the industry for existing 6-MW installations. The primary substructure mass was well captured by the model (maximum error $\simeq 12\%$) within the water depth range from 20–40 m. Although our dataset did not include points below that range, a bilinear extrapolation toward depths of 10 m and hub heights of 90 m produced a 35% underestimation of the existing jacket installations' mass. For depths greater than 40 m, our simulations lacked resolution around 45 m, which is where the currently deepest installations seem to cluster. Nonetheless, the extrapolated jacket mass was within 5% of the installation data.

When compared to data predicted by other consultancies in the industry, a larger scatter was observed. For instance, at water depth of $45\,\mathrm{m}$, our prediction is 35% off that from [54]. One reason for the observed discrepancies is attributed to the optimization strategy employed. Here we simultaneously optimized both tower and substructure; in current industry practice, the substructure is designed independently of the tower.

Another reason for this scatter is attributable to the choices of parameters and design-variable acceptance ranges. In this study, only approximations of turbine parameters (inertial properties, modal acceptance bands, and loads) were available due to the lack of open-source, reference-turbine models.

To verify the effects of site and turbine parameters, we conducted additional optimizations using data from actual turbine projects and specific site metocean records. The loads and geometric properties of a 6-MW turbine were provided by the turbine OEM, whereas the sites were actual NOAA buoy locations. The inputs between these and the original cases mainly differed in system target eigenfrequency, hub height, RNA mass and loads, and, for the deepest site, wave height. The calculated jacket mass agreed well with predicted trends for water depths below $40\,\mathrm{m}$, but in deeper waters the differences in mass predictions were large.

Therefore, one can conclude that when using an engineering approach to cost assessment, technology and metocean data as close as possible to the projects' effective ones are critical to attain reliable techno-economic functions and to build LCOE trends, especially for deep-water sites. In those cases, the inputs to the model should be validated against the expected industry practice and possibly by the turbine OEMs. For more moderate water depths, the bottom-up approach can be assumed as less sensitive to these factors, and the derived functions can be used with greater confidence even with coarser approximations of the input parameters.

6.1. Future Work

LCOE trends will help stakeholders plan appropriately for upcoming U.S. offshore wind developments. As such, the results of this analysis will be further incorporated into lower fidelity models to assess CapEx and LCOE sensitivities to project characteristics (size and turbine spacing), technology (turbine size, substructure and foundation type, electrical infrastructure), and geospatial properties (water depth and distance to shore). The lower fidelity models will demonstrate these trends, allowing for quick, back-of-the-envelope-type analyses that help decision makers target areas for cost and performance improvements [7]. These models, however, will need to account for trade-offs associated with logistics and installation aspects. For instance, having lighter mass piles does not necessarily translate into lower BOS costs because longer but thinner piles may require a longer installation time and therefore higher costs.

It is recommended that future research gather more accurate site and turbine parameters and expand the fidelity of the model. In particular, future work shall address fatigue analysis either through incorporating such capabilities within the tool itself or, more likely, by interfacing the tool more closely with a full aero-elastic module that is also integrated in the systems engineering model set. In parallel, a thorough uncertainty quantification should be performed both on the data inputs and model characteristics.

As we have shown, the model results are highly sensitive to the choices of the input parameters in deep waters ($> 40\,\mathrm{m}$). It is therefore crucial to incorporate reliable metocean conditions for deeper sites, and hurricane data for regions such as the South Atlantic and Gulf of Mexico. For these regions, robustness checks against a 500-yr storm must also be added to the analysis [23, 56]. Additionally, other parked and fault conditions that might be important for the substructure design should be assessed.

Future studies should make use of more complete datasets, wherein turbine parameters and loads are derived from complete aeroelastic analyses. The involvement of the turbine OEMs is necessary to have an accurate portrayal of the turbine-loading scenarios, but this has been historically difficult to achieve because of intellectual property protection concerns. For instance, the effect of changes in the modal constraint on the overall structural mass should be assessed based on what OEMs deem feasible for the near-future controller technology. This aspect should be studied within the context of codesign, where one could leverage control design strategies to reduce mass even further, for example, by permitting resonance frequencies to be within the operational rotor range. Toward this end, we intend to work on the development of

new, thorough, reference wind turbine models that can be readily scaled for sensitivity analyses and technology assessment studies.

Future research can enhance the model capabilities by including revised hydrodynamics, fatigue, and pile verification. The dataset will then be augmented with refined cost curves for select sites, for which metocean conditions are known with accuracy, and for newly installed projects, as they come online and available, to further tune and validate the model. Finally, innovative designs (such as three-legged jackets) should also be explored in detail.

ACKNOWLEDGEMENT

This work was supported by the U.S. Department of Energy (DOE) under Contract No. DE-AC36-08GO28308 with the National Renewable Energy Laboratory. Funding for the work was provided by the DOE Office of Energy Efficiency and Renewable Energy, Wind and Water Power Technologies Office. We acknowledge George Scott of NREL for providing the buoy metocean data.

REFERENCES

1. US Department of Energy. Wind Vision: A New Era for Wind Power in the United States. *DOE pub. DOE/GO-102015-4557* 2015.
2. Elliott D, Schwartz M, Haymes S, Heimiller D, Musial W. Assessment of offshore wind energy potential in the United States. *National Renewable Energy Laboratory Poster PO-7A20-51332*, NREL, Golden, CO 2011.
3. Musial W, Butterfield S. Deepwater offshore wind technology research requirements. *WindPower 2005*, AWEA: Denver, CO, 2005.
4. Musial WD, Butterfield S, Ram B. Energy from offshore wind. *Offshore Technology Conference*, Houston, TX, 2006; 1888–1898.
5. De Vries W, Vemula N, Passon P, Fischer T, Kaufer D, Matha D, Schmidt B, Vorpahl F. Final report WP4.2: Support structure concepts for deep water sites. *Technical Report UpWind_WP4_D4.2.8_Final Report*, Delft University of Technology, Stevinweg 1, Delft, The Netherlands 2011. Project Upwind Contract No. 019945 (SES6).
6. Mone C, Smith A, Maples B, Hand M. Cost of wind energy review. *Technical Report TP-5000-63267*, NREL, Golden, CO 2015.
7. Lozano-Minguez E, Kolios A. Multi-criteria assessment of offshore wind turbine support structures. *Renewable Energy* November 2011; **36**(11):2831–2837.
8. Smith A, Stehly T, Musial W. 2014-2015 offshore wind technologies market report. *Technical Report NREL/TP-5000-64283*, NREL, Golden, CO September 2015.
9. Trust TC. Offshore wind power: Big challenge, big opportunity - maximising the environmental, economic and security benefits. *Technical Report Rept CTC743*, The Carbon Trust, UK 2008. 112 pp.
10. BVG Associates. Offshore wind cost reduction pathways technology work stream. *Technical report*, The Crown Estate May 2012.
11. Kaiser MJ, Snyder BF. *Offshore Wind Energy Cost Modeling - Installation and dec*. Green Energy and Technology, Springer-Verlag: London, 2012. 235 pp.
12. Dykes K, Ning A, King R, Graf P, Scott G, Veers P. Sensitivity analysis of wind plant performance to key turbine design parameters. *AIAA SciTech 2014 - 32nd ASME Wind Energy Symposium*, National Harbor, MD, 2014; 697–722.
13. Ning SA, Damiani R, Moriarty PJ. Objectives and constraints for wind turbine optimization. *Journal of Solar Energy Engineering* June 2014; **136**(4):041 010–041 010–12, doi:10.1115/1.4027693. 12 pp.

14. Dykes K, Meadows R, Felker F, Graf P, Hand M, Lunacek M, Michalakes J, Moriarty P, Musial W, Veers P. Applications of systems engineering to the research, design, and development of wind energy systems. *Technical Report NREL/TP-5000-52616*, NREL, Golden, Colorado December 2011.
15. Damiani R. JacketSE—an offshore wind turbine jacket sizing tool—theory manual. *Technical Report NREL/TP-5000-65417*, NREL, Golden, CO January 2016.
16. Damiani R, Song H. A jacket sizing tool for offshore wind turbines within the systems engineering initiative. *Offshore Technology Conference*, Offshore Technology Conference: Houston, Texas, USA, 2013, doi:http://dx.doi.org/10.4043/24140-MS.
17. Cordle A, McCann G, de Vries W. Design drivers for offshore wind turbine jacket support structures. *ASME 2011 30th International Conference on Ocean, Offshore and Arctic Engineering—OMAE2011*, ASME: Rotterdam, The Netherlands, 2011; 419–428.
18. Zwick D, Schafhirt S, Brommundt M, Muskulus M, Narasimhan S, Mechineau J, Haugsen P. Comparison of different approaches to load calculation for the OWEC Quattropod jacket support structure. *J. of Physics: Conference Series* 2014; **555**(012110), doi:doi:10.1088/1742-6596/555/1/012110.
19. Molde H, Zwick D, Muskulus M. Simulation-based optimization of lattice support structures for offshore wind energy converters with the simultaneous perturbation algorithm. *J. of Physics: Conference Series* 2014; **555**(012075), doi:doi:10.1088/1742-6596/555/1/012110.
20. Pender MJ. Aseismic pile foundation design analysis. *Bulletin of the New Zealand National Society for Earthquake Engineering* March 1993; **26**(1):49–159.
21. Matlock H, Reese LC. Generalized solutions for laterally loaded piles. *J. Soil Mechanics & Foundation Division* 1960; **86**(5):91–97.
22. Bowles JE. *Foundation Analysis and Design*. 5th edn., The McGraw-Hill Companies, Inc., 1997. 1168 pp.
23. API. Planning, designing and constructing fixed offshore platforms - working stress design November 2014. API Recommended Practice 2A-WSD.
24. IEC. 61400-3 wind turbines—part 3: Design requirements for offshore wind turbines 2009.
25. DIN. Din 1055-4 (2005-03): Action on structures—part 4: Wind loads March 2005.
26. Eurocode 1: Actions on structures—part 1-4: General actions—wind actions April 2010.
27. SEI. *Minimum Design Loads for buildings and other structures*. American Society of Civil Engineers, 2005. ASCE Standard, ASCE/SEI 7-05.
28. SEI. *Minimum Design Loads for buildings and other structures (ASCE/SEI 7-10)*. 3rd printing edn., American Society of Civil Engineers: 1801 Alexander Bell Drive, Reston, Virginia 20191, 2010. ASCE Standard, ASCE/SEI 7-10.
29. Burton T, Sharpe D, Jenkins N, Bossanyi E. *Wind Energy Handbook*. 1st edn., John Wiley and Sons, Inc.: 111 River St., Hoboken, NJ 07030, USA, 2005.
30. Murtagh PJ, Basu B, Broderick BM. Gust response factor methodology for wind turbine tower assemblies. *J. of Structural Engineering* January 2007; **133**(1):139–144, doi:http://dx.doi.org/10.1061/(ASCE)0733-9445(2007)133:1(139).
31. Chakrabarti SK. *Hydrodynamics of Offhore Structures*. WIT Press: Southampton, UK, 1987. 440 p.
32. ISO. 19901-1:2005 (modified) - petroleum and natural gas industries – specific requirements for offshore structures – part 1: Metocean design and operating considerations November 2014. ANSI/API Recommended Practice 2MET.
33. Gavin HP. User manual and reference for Frame3DD: A structural frame analysis program November 2010. URL https://nees.org/resources/1650/download/frame3dd.pdf.
34. Timoshenko S, Goodier J. *Theory of elasticity*. 3rd edn., Engineering societies monographs, McGraw-Hill: New York, USA, 1970. 567 pp.
35. Panzer H, Hubele J, Eid R, Lohmann B. Generating a parametric finite element model of a 3d cantilever timoshenko beam using MATLAB. *Technical Reports on Automatic Control TRAC-4*, Technische Universitat Munchen November 2009.

36. IEC. 61400-1. wind turbines—part 1: Design requirements 2005.
37. Germanischer Lloyd. Guideline for the certification of offshore wind turbines 2012.
38. DNV. Design of offshore wind turbine structures 2 2013.
39. ISO. 19902:2007 - petroleum and natural gas industries – fixed steel offshore structures 2007.
40. ANSI. Specification for structural steel buildings June 2010. 3rd printing: 2013.
41. Eurocode 3: Design of steel structures—part 1-1: Genstructures and rules for buildings 2005.
42. ABS. Guide for buckling and ultimate strength assessment for offshore structures February 2014.
43. DNV. Offshore standard DNV-OS-C501 - composite components October 2010.
44. Chakrabarti SK ((ed.)). *Handbook of Offshore Engineering*. Elsevier: The Boulevard Langford Lane, Kidlington, Oxford OX5 lGB, UK, 2005. 2 volume set –1321 pp.
45. Powell M. A direct search optimization method that models the objective and constraint functions by linear interpolation. *Advances in Optimization and Numerical Analysis – Proceedings of the sixth workshop on optimization and numerical analysis*, Gomez S, Hennart J (eds.), no. 275 in Mathematics and its Applications, Kluwer Academic Publishers: Oaxaca, Mexico, 1994. Pp. 51-67.
46. Gill PE, Murray W, Saunders MA. SNOPT: An SQP algorithm for large-scale constrained optimization. *SIAM REVIEW* 2005; **47**(1):99–131, doi:10.1137/S0036144504446096.
47. Van der Tempel J. Design of support structures for offhore wind turbines. PhD Thesis, TU Delft, Stevinweg 1, 2628 CN Delft, The Netherlands April 2006. 209 pp.
48. ASTM. ASTM A992 / A992M - 11(2015) standard specification for structural steel shapes 2015. URL www.astm.org.
49. Germanischer Lloyd. Guideline for the certification of offshore wind turbines 2005.
50. Eurocode 3: Design of steel structures—part 1-6: General rules—supplementary rules for the shell structures 1993.
51. API. Planning, designing and constructing fixed offshore platforms - load and resistance factor design May 2003. Withdrawn.
52. Jonkman J, Butterfield S, Musial W, Scott G. Definition of a 5-MW reference wind turbine for offshore system development. *Technical Report NREL/TP-500-38060*, NREL, Golden, CO Februaury 2015.
53. Seidel M. 6 MW turbines with 150m+ rotor diameter- what is the impact on substructures? *11th German Wind Energy Conference- DEWEK 2012*, Bremen, Germany, 2012.
54. GL Garrad Hassan. Expected offshore wind farm balance of station costs in the united states 2012. NREL's Subcontractor's report.
55. ABS. Guide for building and classing - bottom-founded offshore wind turbine installations January 2013. URL http:\//www.eagle.org/eagleExternalPortalWEB\/ShowProperty\/BEA%20Repository\/Rules&Guides\/Current\/176_BOWTI\/Guide, revised July 2014.
56. AWEA. Offshore compliance recommended practices recommended practices for design, deployment and operation of offshore wind turbines in the united states 2012.